



Experimental Study of Wave Attenuation Across an Artificial Salt Marsh

Scott Baker^{1*}, Enda Murphy¹, Andrew Cornett^{1,2} and Paul Knox¹

¹Ocean, Coastal, and River Engineering Research Centre, National Research Council, Ottawa, ON, Canada, ²Department of Civil Engineering, University of Ottawa, Ottawa, ON, Canada

OPEN ACCESS

Edited by:

Tori Tomiczek,
United States Naval Academy,
United States

Reviewed by:

M. Luisa Martínez,
Instituto de Ecología (INECOL),
Mexico
Mireille Escudero,
National Autonomous University of
Mexico, Mexico
Jord J. Warmink,
University of Twente, Netherlands

*Correspondence:

Scott Baker
scott.baker@nrc-cnrc.gc.ca

Specialty section:

This article was submitted to
Coastal and Offshore Engineering,
a section of the journal
Frontiers in Built Environment

Received: 10 March 2022

Accepted: 17 May 2022

Published: 08 June 2022

Citation:

Baker S, Murphy E, Cornett A and
Knox P (2022) Experimental Study of
Wave Attenuation Across an Artificial
Salt Marsh.
Front. Built Environ. 8:893664.
doi: 10.3389/fbuil.2022.893664

Scaled laboratory experiments were conducted to investigate the effectiveness of marsh vegetation in dissipating wave energy and reducing wave overtopping discharges at the crest of a dyke located immediately landward of the marsh. Model dyke and marsh platform features, loosely based on archetypes found in Atlantic Canada, were constructed in a wave basin at 1:20 scale and exposed to a broad range of waves and water level conditions. The 2D experiments were conducted using idealized surrogate vegetation (both rigid and flexible), and the model setup featured four parallel flumes which enabled four alternative configurations to be investigated simultaneously. The experiments investigated the sensitivity of wave attenuation and overtopping to the length of the vegetation field, vegetation characteristics (stem density, height, and flexibility) and varying water levels and wave conditions. The study outputs have helped to address knowledge gaps and provide evidence to support and inform broader use of hybrid marsh-dyke systems and managed dyke realignment to help manage flood and erosion risk and improve coastal resilience in Canada and internationally. This research confirmed the benefit of tidal flats hosting coastal marshes for attenuating waves, reducing overtopping volumes and lessening damage to dyke structures. As expected, taller and denser marshes were more effective in attenuating wave energy for a given marsh width.

Keywords: wave attenuation by vegetation, salt marsh, physical modelling, artificial vegetation, flood and erosion risk

1 INTRODUCTION

The global risk associated with coastal flooding and erosion has increased substantially over the past several decades, as a consequence of population growth, development in coastal zones and climate change effects including sea-level rise (Jongman, 2018). Projections for the 21st century suggest that these trends will continue (Muis et al., 2020), and, in the absence of intervention or adaptation, the exposure of people and valued assets to episodic coastal flooding could increase by nearly half (Kirezci et al., 2020). There is a large and growing body of evidence surrounding the benefits of natural and nature-based solutions (NBS) as viable alternatives or complements to conventional (hard) engineering shore protection measures (Browder et al., 2019; Bridges et al., 2014; Spalding et al., 2014; Sutton-Grier et al., 2015; Moudrak et al., 2018; Sutton-Grier et al., 2018; Bridges et al., 2021). In particular, the value provided by coastal wetlands or marshes in supporting flood and erosion risk management objectives has been well demonstrated (Costanza et al., 2008; Arkema et al., 2013; Narayan et al., 2017; Piercy et al., 2021).

Coastal marsh systems deliver flood and erosion risk management benefits by attenuating waves and storm surges (Barbier et al., 2011), attracting and retaining sediment (Shepard et al., 2011), and by providing hydraulic storage (Barbier et al., 2011; Shepard et al., 2011; Webb et al., 2018); while at the same time providing a host of co-benefits (Spalding et al., 2014; Pontee et al., 2016; Piercy et al., 2021). Unlike hard structures, coastal marshes can self-adapt to rising sea levels under the right settings (Spalding et al., 2014; Piercy et al., 2021). For example, if sediment supply and accretion rates exceed sediment losses caused by erosion or other mechanisms, marsh growth can offset relative sea-level rise (Barbier et al., 2011; Pontee et al., 2016). Nature-based solutions for coastal hazard risk management that incorporate marsh systems can be implemented through conservation and restoration of existing or degraded marsh systems, landward realignment of hard defences resulting in restoration or generation of new marshes (e.g., managed dyke realignment), and construction of new wetland features (Piercy et al., 2021). The latter two forms of intervention (managed realignment and marsh construction) typically involve hybrid solutions (Spalding et al., 2014; Sutton-Grier et al., 2015; Pontee et al., 2016; Vuik et al., 2016; Jongman, 2018; Vuik et al., 2018), whereby hard structures are integrated with marsh and other vegetation features to provide flood and erosion risk management function. In the case of hybrid dyke-marsh systems, the presence of a foreshore salt marsh can reduce the failure probability of a landside dyke (Vuik et al., 2018), and reduce the costs of dyke maintenance and upgrades (Jongman, 2018). However, the lack of data and rigorous analyses demonstrating the performance and limitations of such hybrid NBS under a variety of environmental settings and metocean conditions remains a barrier to uptake (Sutton-Grier et al., 2015; Morris et al., 2018).

Coastal communities and infrastructure in Canada are vulnerable to flooding and erosion caused by water level and wave extremes (Lemmen et al., 2016), and the risks are expected to increase over the coming decades due to urbanization, rising sea levels, declining sea ice cover, and shifting weather patterns associated with climate change (Bush and Lemmen, 2019). The risk to coastal communities, including damage to infrastructure, is one of the top climate change risks facing Canada (Council of Canadian Academies, 2019). Some coastal regions of Canada have a legacy of dyke construction, which has facilitated settlement, population growth and agricultural activities in low-lying coastal regions (van Proosdij et al., 2013; Sherren et al., 2019). Many of these older dykes now provide a certain level of protection to communities, valued land and assets from coastal hazards (Barron et al., 2012; van Proosdij et al., 2013; Doberstein et al., 2019), although many have been poorly maintained and are in need of repair (van Proosdij et al., 2013). The resources demanded to maintain and upgrade this ageing infrastructure stock are substantial (Barron et al., 2012; Doberstein et al., 2019; Sherren et al., 2019), particularly in the face of rising relative sea levels. In some places, the dykes have contributed to loss of valued salt marsh ecosystems (Virgin et al., 2020). Over-reliance on dykes as a sole flood protection strategy can also introduce vulnerabilities, for example by creating a false perception of risk and encouraging development in flood-prone

areas, or leading to catastrophic consequences in the event of a dyke breach or failure (Jongman, 2018). Natural or nature-based features, such as marshes and barrier islands, can act in concert with dykes as part of multiple-lines-of-defence strategies to increase engineering redundancy, enhance the level of flood protection provided, and reduce the costs of dyke maintenance or upgrades (Barron et al., 2012; Jongman, 2018). Empirical field evidence of the effectiveness of hybrid dyke-marsh systems is being developed for a number of managed realignment pilot projects in Atlantic Canada, which were typically implemented by: (i) constructing new dykes landward of legacy agricultural dykes, and (ii) breaching the old dykes to restore tidal flows and facilitate marsh restoration (Sherren et al., 2019; Virgin et al., 2020). Although managed dyke realignment and hybrid-dyke marsh systems are common approaches to flood and erosion risk management in many of the world's coastal regions, such solutions still pose some risk in the Canadian context. This is due, in part, to uncertainty surrounding the performance of these nature-based solutions in diverse Canadian coastal environmental settings, which are characterized by extreme variability in regional climates, tidal ranges, rates of relative sea-level rise, and exposure to wave energy. An improved understanding of the performance of hybrid dyke-marsh systems under a broad range of conditions is needed to guide applications in Canada, and in other regions where uptake has been relatively low.

This paper describes a series of scaled laboratory experiments conducted to investigate the hydraulic performance of hybrid marsh-dyke systems, and in particular examine the effectiveness of coastal marshes in dissipating wave energy and reducing wave overtopping under a broad range of wave and water level conditions representative of Canadian coastal regions. The experiments used physical modelling to investigate dyke and marsh platform features typically found in the Tantramar Marsh on the Chignecto Isthmus in the upper Bay of Fundy, shared by the Canadian provinces of New Brunswick and Nova Scotia, which features *Spartina alterniflora* (smooth cordgrass) vegetation. It is worth noting that the upper Chignecto Bay can be characterized as a macro-tidal environment where high tide typically reaches from 9.5 to 14 m above chart datum. In these experiments, the marsh vegetation was represented using both rigid and flexible artificial or surrogate vegetation designed to approximate the effect of real vegetation on wave attenuation. The experimental study is unique in several respects:

- Testing was conducted with identical wave conditions in four identical flumes arranged side-by-side, so that the effect of controlled changes in various marsh properties including surrogate plant density, stem height, stem flexibility and marsh width (in the direction of wave propagation) could be directly assessed by comparing data and observations obtained at the same time from neighbouring flumes.
- In contrast with many previous studies which focused on wave-plant interaction at full scale or near full scale, this study focused on assessing the changes in wave properties across a 4.75 m wide (95 m wide at full scale) artificial coastal marsh and their interaction with a dyke located

immediately landward of the marsh. The effect of various marsh properties and characteristics on the wave attenuation, the volume of wave overtopping and extent of damage (to the dyke) was assessed.

- The artificial marsh's effect on wave attenuation was investigated over a broad range of significant wave height (H_{m0}), peak period (T_p) and local water depth (h) or plant submergence.
- Although the experiments were conducted at 1/20 scale, the wave conditions included significant wave heights and periods up to 0.15 m and 3.35 s, representing full scale conditions with $H_{m0} = 3$ m and $T_p = 15$ s, which are believed to be more energetic than those considered in previous experimental research involving coastal marshes.

This study used an artificial marsh to provide new information on the performance of marsh-dyke systems in a broad range of wave and water level conditions, and the sensitivity of wave attenuation, wave overtopping and damage to variables such as plant density, plant height (submergence), stem flexibility, marsh width, significant wave height, peak period and local water depth. The methods and results described in the paper may be useful to others interested in representing coastal marshes in physical or numerical models of coastal processes and shoreline developments incorporating natural and nature-based features.

Section 2 summarizes the results from a literature review on how marsh vegetation has been represented in past laboratory experiments, while **Section 3** introduces the existing theory and formulae for predicting wave attenuation by marsh vegetation. New 2D experiments conducted at 1/20 scale with coastal marshes comprised of surrogate vegetation fronting dyke structures are described in **Section 4**. **Section 5** presents an analysis and discussion of the new experimental data, in which many of the formulae presented in **Section 3** are used, while the main conclusions from this work are summarized in **Section 6**.

2 PAST REPRESENTATION OF MARSH VEGETATION IN PHYSICAL EXPERIMENTS

The experiments discussed in the present work were conducted using idealized surrogate vegetation representing *S. alterniflora*. The stem densities, heights and diameters of the model vegetation were selected based on findings in literature (Percy, 2000; Lightbody and Nepf, 2006; Cranford et al., 2008; Anderson and Smith, 2014; Nepf et al., 2017; Feagin et al., 2019; Pinsky et al., 2021). For this study, the average stem diameter and height of *S. alterniflora* was taken as 8.7 mm and 1.80 m respectively, though these values depend on the season, the geographic location, and a number of environmental factors.

Some species of vegetation may be successfully represented using rigid elements such as aluminum rods (mangroves) or wooden dowels (salt marsh), despite demonstrating some degree of flexibility in reality (Wu et al., 2011; Arkema et al., 2013; Maza et al., 2019; van Veelen et al., 2020). A combined field-numerical study demonstrated that *S. alterniflora* can be reasonably modelled as a rigid cylinder (Jadhav et al., 2013). Similarly,

Augustin et al. (2009) modelled *S. alterniflora* using both rigid and flexible elements and found that the two models produced similar attenuation effects for the tested flow conditions. Thus, the appropriate selection of rigid versus flexible elements may depend on the experimental hydrodynamic conditions.

These elements are often selected to mimic the geometric parameters of the target vegetation, including stem/blade length, width, diameter and planting density (Arkema et al., 2013; Anderson and Smith, 2014; Ozeren et al., 2014; Maza et al., 2019). For small-scale physical models with surrogate vegetation, stem diameters should only be downscaled if flows remain in the rough-turbulent range, as overly small stem diameters can lead to overly small stem Reynolds numbers and significant distortions in drag coefficient (Blackmar et al., 2012).

Table 1 presents a concise summary of previous experimental studies conducted with both real and surrogate marsh vegetation.

Markov (2021) conducted an extensive review of state-of-the-art physical and numerical modelling research in the use of vegetation for coastal protection. Based on the reviewed body of literature, a number of knowledge gaps and recommendations for future research were identified, in particular: developing knowledge of species-specific attenuation capacity considering seasonal variation in biomass and plant characteristics; comparing small- and large-scale models to quantify scaling effects, addressing uncertainties associated with modelling NBS at a small-scale and thus allowing practitioners to better interpret the results of small-scale testing for the design of NBS; testing a wider range of hydrodynamic conditions to determine the impact of wave period on attenuation capacity, with the aim to address presently conflicting results from previous experimental works; perform further testing on stem density and arrangement.

In summary, although there have been numerous previous experimental studies of wave-vegetation interaction, the majority of studies were conducted at prototype or near-prototype scale, and therefore considered processes over a rather limited spatial extent and with a narrow range of conditions (waves and water levels). In addition, much of the previous work dealt only with the effect of vegetation itself, without looking at the broader application of combined systems (e.g., vegetation fronting coastal dykes). While this approach limits or eliminates model scaling effects, knowledge gaps remain surrounding application of the results to real-world situations and larger spatial extents. The absence of studies covering a broad range of environmental conditions and longer sections of marsh is a barrier to understanding how salt marsh creation or restoration can be practically implemented to provide optimal flood and erosion risk management function. As described above, a number of challenges exist for using live vegetation in experimental studies. Real vegetation cannot be used for assessing performance at model scale, whereas the use of surrogate vegetation provides the ability to change the model scale as needed and study processes over larger areas. In this work, a scaled physical modelling approach in a large wave basin facility is used to address some of these gaps and better inform design of hybrid marsh-dyke systems.

TABLE 1 | Summary of previous experimental studies with marsh vegetation.

Study	Species, model material	Testing variables	Observed variables	Key findings
Anderson and Smith (2014)	<i>Spartina alterniflora</i> , polyolefin tubing	<ul style="list-style-type: none"> • Stem density • Submergence • Wave height • Wave period 	<ul style="list-style-type: none"> • Wave attenuation 	<ul style="list-style-type: none"> • Wave attenuation appeared most dependent on stem density and ratio of stem length to water depth • Wave attenuation increased slightly with wave height, no clear trend with respect to wave period
Lightbody and Nepf (2006)	<i>Spartina alterniflora</i>	<ul style="list-style-type: none"> • Field measurements 	<ul style="list-style-type: none"> • Stem frontal area • Velocity • Vertical diffusion • Longitudinal dispersion 	<ul style="list-style-type: none"> • Vegetation volumetric frontal area peaked ~10 cm from bed • Velocity profile varied inversely with canopy drag (i.e., velocity is min. where frontal area is max.)
Augustin et al. (2009)	<i>Spartina alterniflora</i> , wooden dowels, polyethylene foam tubing	<ul style="list-style-type: none"> • Water depth • Stem density • Wave height • Wave period 	<ul style="list-style-type: none"> • Wave attenuation 	<ul style="list-style-type: none"> • Laboratory data analyzed using linear wave theory to quantify bulk drag coefficients and with nonlinear Boussinesq model to determine numerical friction factors to better represent wetland vegetation
Koftis et al. (2013)	<i>Posidonia oceanica</i> , PVC stem and leaves	<ul style="list-style-type: none"> • Stem density • Submergence 	<ul style="list-style-type: none"> • Wave attenuation • Wave-induced velocities 	<ul style="list-style-type: none"> • Calculated vs. measured wave heights found to be in agreement • Wave orbital velocities shown to be significantly attenuated inside the meadow and just above flume bed • Submerged vegetation attenuated mostly longer waves
Pinsky et al. (2013)	Kelp, mangrove, marsh and seagrass species	<ul style="list-style-type: none"> • Re-analysis of existing wave attenuation studies 	<ul style="list-style-type: none"> • Wave attenuation 	<ul style="list-style-type: none"> • Much of the variation in wave attenuation explained by differences in vegetation characteristics and change in bulk drag with flow conditions • Vegetation can exert substantial drag on passing waves, but bulk drag coefficient declines in flow conditions characterized by high Reynolds numbers
Ozereen et al. (2014)	<i>Spartina alterniflora</i> and <i>Juncus roemerianus</i> , live plants, wooden dowels, EPDM foam-rubber cords	<ul style="list-style-type: none"> • Vegetation type • Stem density • Plant height • Wave height • Wave period 	<ul style="list-style-type: none"> • Wave attenuation 	<ul style="list-style-type: none"> • C_D did not depend significantly on the relative submergence • Drag coefficients were higher for live vegetation species than for rigid and flexible surrogate vegetation • Vertical variation of plant density strongly influenced the drag coefficient
Lara et al. (2016)	<i>Puccinellia maritima</i> and <i>Spartina anglica</i> , live plants	<ul style="list-style-type: none"> • Wave height • Wave period • Currents • Water depth • Stem density 	<ul style="list-style-type: none"> • Wave attenuation 	<ul style="list-style-type: none"> • Challenges of employing live vegetation: selection of appropriate species; source, quantity and survivability of selected plants; suitability of substrate; experimental setup to simulate natural conditions; plant degradation throughout the experiment; hydraulic characteristics to be tested and measurement techniques; plant response to hydraulic loading; plant characteristics; logistics and operation to conduct a large-scale experiment using real vegetation

(Continued on following page)

TABLE 1 | (Continued) Summary of previous experimental studies with marsh vegetation.

Study	Species, model material	Testing variables	Observed variables	Key findings
Houser et al. (2015)	<i>Thalassia testudinum</i> , wooden dowels, cable ties, polyethylene ribbon	<ul style="list-style-type: none"> • Blade rigidity • Wave height • Wave period • Water depth 	<ul style="list-style-type: none"> • Wave attenuation 	<ul style="list-style-type: none"> • Drag coefficient exhibited strong dependency on the flexibility of individual blades • Flexible vegetation had relatively small drag coefficient compared to rigid vegetation • Flexible vegetation provides little to no shoreline protection, except where the vegetation field is extensive and high density
Wu and Cox (2015a); Wu and Cox (2015b)	wooden dowels (no specific species)	<ul style="list-style-type: none"> • Vertical variation in vegetation density • Wave nonlinearity 	<ul style="list-style-type: none"> • Wave attenuation 	<ul style="list-style-type: none"> • Damping factor dependent on the wave steepness • Damping factor can increase by a factor of two when the wave steepness approximately doubles • Highlighted the effect of vertical biomass distribution which can result in changes in C_D
Losada et al. (2016)	<i>Spartina anglica</i> and <i>Puccinellia maritime</i> , live vegetation	<ul style="list-style-type: none"> • Wave height • Wave period • Plant density • Water depth • Currents 	<ul style="list-style-type: none"> • Wave attenuation 	<ul style="list-style-type: none"> • New analytical formulation for evaluation of wave damping under combined effect of waves and both following and opposing currents, suggested for implementation in phase-averaged and phase-resolving numerical models of wave propagation
Vuik et al. (2016)	<i>Spartina anglica</i> and <i>Scirpus maritimus</i>	<ul style="list-style-type: none"> • Field measurements • Numerical modelling 	<ul style="list-style-type: none"> • Wave attenuation 	<ul style="list-style-type: none"> • Numerical model appeared capable of reproducing the observed decay in wave height over the salt marsh, applied to compute the reduction of incident wave height on a dyke for various foreshore configurations • Vegetated foreshores can be considered promising supplement to conventional engineering methods for dyke reinforcement
Sonnenwald et al. (2019)	rigid cylinders (no specific species)	n/a	<ul style="list-style-type: none"> • Evaluated several practical engineering functions for estimating bulk drag coefficient 	<ul style="list-style-type: none"> • Estimates of C_D were compared to a range of experimental data from previous studies wherein a frontal area approach was used for selecting the stem diameter and spacing • Estimates of C_D utilizing the re-parametrization presented match the experimental data better than estimates of C_D made using the other functions evaluated
Lei and Nepf (2019)	<i>Various seagrass species</i> , LDPE film	<ul style="list-style-type: none"> • Plant morphology • Plant flexibility • Stem density • Water depth • Wave height • Wave period 	<ul style="list-style-type: none"> • Wave attenuation 	<ul style="list-style-type: none"> • Validated new model to predict dissipation of wave energy over submerged meadow of flexible plants • Vegetation drag and thus wave decay are diminished relative to that for a fully rigid blade of the same geometry
Keimer et al. (2021)	rigid PVC rods (no specific species)	<ul style="list-style-type: none"> • Wave height • Wave period • Water depth • Plant height 	<ul style="list-style-type: none"> • Wave attenuation • Wave run-up 	<ul style="list-style-type: none"> • Vegetated foreshores contribute to a mean wave attenuation of 9% • Wave run-up reduction up to 16.5% observed with decreasing water depths and increasing vegetation heights • Authors noted a number of topics for further investigation regarding the eco-hydraulic effects of foreshore vegetation

3 PREDICTION OF WAVE ATTENUATION BY VEGETATION

As described in many previous studies [e.g., 1,35,44], the prediction of wave attenuation over a coastal marsh can be based on the energy conservation equation. Assuming a flat bed, linear wave theory, invariant quantities with depth, and rigid vegetation (no swaying motion), the regular wave height profile along the vegetation field can be written as (Dalrymple et al., 1984):

$$\frac{H}{H_i} = \frac{1}{1 + \beta x} \quad (1)$$

where H_i is the incident wave height; H is the wave height within the vegetation field (at location x); and β is the damping coefficient for regular wave trains. Mendez and Losada (2004) extended this formulation for non-breaking random waves over constant depth assuming a Rayleigh distribution and deriving the wave height evolution as a function of the root-mean-square wave height as :

$$\frac{H_{rms}}{H_{rms,i}} = \frac{1}{1 + \beta' x} \quad (2)$$

And

$$\beta' = \frac{1}{3\sqrt{\pi}} H_{rms,i} C_D a k_p \frac{\sinh(k_p s h)^3 + 3 \sinh(k_p s h)}{\sinh(k_p h) [\sinh(2k_p h) + 2k_p h]} \quad (3)$$

where $H_{rms,i}$ is the root-mean-square (RMS) height of the incident waves; H_{rms} is the RMS wave height inside the vegetation field (at location x); C_D is the depth-averaged spatial mean bulk drag coefficient; $a = D_v N_v$ is the total frontal plant area per unit volume; D_v is the stem diameter; N_v is the vegetation stem density; h_v is the vegetation height; $k_p = 2\pi/L_p$ is the wave number; L_p is the wavelength associated with the peak period (T_p); h is the water depth; and $s = h_v/h$ for submerged ($h_v < h$) and unity for emergent ($h_v > h$) vegetation.

Drag coefficients, energy dissipation and wave attenuation are a strong function of Reynolds number and Keulegan–Carpenter number (Keulegan and Carpenter, 1958). The stem Reynolds number is calculated as :

$$Re = \frac{u_c D_v}{\nu} \quad (4)$$

where ν is the kinematic viscosity of seawater ($1.44 \times 10^{-6} \text{ m}^2/\text{s}$ at 8°C , the average temperature of Atlantic Canadian waters); and u_c is the characteristic velocity acting on the plant. The characteristic velocity is defined as :

$$u_c = \frac{\bar{H}_{rms}}{2} \omega_p \frac{\cosh(ksh)}{\sinh(kh)} \quad (5)$$

where \bar{H}_{rms} is the average root-mean-square wave height across the vegetation field; and ω_p is the peak wave angular frequency.

The Keulegan–Carpenter number :

$$KC = \frac{u_c T_p}{D_v} \quad (6)$$

Describes the relative importance of drag forces versus inertia forces for objects in an oscillatory fluid flow. For relatively small values of KC , the water particle displacements become

comparable to the stem diameter, and inertia force dominates. For larger values of KC , water particle displacements are much larger than the stem diameter, leading to flow separation and vortex shedding, and drag force becomes increasingly important. Some researchers (Ozeren et al., 2014; Wu and Cox, 2015b) have shown dependence on the KC number. Following Sonnenwald et al. (2019), the drag coefficient can be written as :

$$C_D = 2 \left(\frac{6475 D_v + 32}{Re} + 17 D_v + 3.2 \phi + 0.50 \right) \quad (7)$$

where ϕ is the solid volume fraction = $a D_v \pi/4$.

4 EXPERIMENTAL METHODS AND MATERIALS

4.1 Experimental Setup

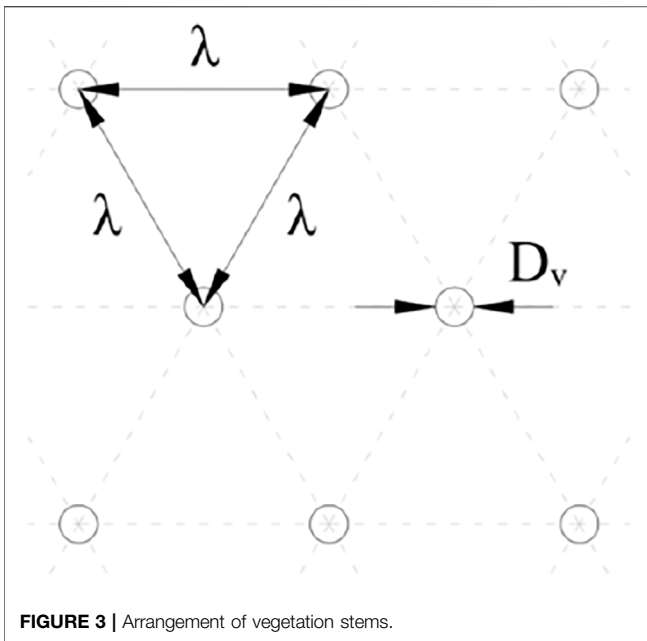
The present study was conducted in the National Research Council of Canada's (NRC) 63 m long by 14 m wide by 1.5 m tall Coastal Wave Basin (CWB). The CWB is equipped with a computer-controlled wave machine capable of generating irregular long-crested waves with significant wave heights up to ~ 0.35 m (at model scale). The active wave absorption feature was not enabled during this study.

A length scale of 1/20 was adopted for the experiments, and Froude scaling was used to relate most (but not all) conditions in the model to corresponding conditions at full scale. The 1/20 scale factor, together with the chosen wave conditions and the fact that the surrogate plant stems in the model were purposely over-sized, ensured that the wave-driven flows around the model vegetation and model armour stones on the dyke surface remained rough-turbulent at all times, as in nature. Preserving rough-turbulent flow in the model was essential to minimizing scale effects and preserving the realism of the wave-plant and wave-structure interactions in the physical model.

The 14 m wide CWB was subdivided into four separate 1.22 m wide flumes by erecting parallel masonry block walls (see **Figure 1**). This setup created four identical test flumes and allowed four different marshes to be built and evaluated at the same time, one per flume, with identical incident wave conditions in front of each marsh. Each flume included an identical scaled reproduction of the typical sloping foreshore along the edge of the Tantram Marsh on the Chignecto Isthmus, as well as an idealized model dyke structure (see **Figure 2**). A $\sim 1\text{V}:11\text{H}$ foreshore slope followed by a 4.75 m long (95 m at full scale) horizontal tidal flat was created by rigidly securing thick plywood sheets to the flume walls.

The floor of the wave basin at the toe of the sloping foreshore was assigned an elevation of -0.18 m (corresponding to -3.50 m at full scale), while the tidal flat elevation was $+0.27$ m ($+5.40$ m at full scale). Water depths on the tidal flat in this study ranged from 0.05 to 0.12 m (1.0 – 2.4 m at full scale). The bathymetry helped to ensure that wave conditions at the edge of the marsh in the physical model, including the distribution of wave heights and the percentage of breaking and broken waves, was similar to head-on wave conditions at the edge of typical marshes in upper Chignecto Bay.

Marshes comprised of *S. alterniflora* were simulated on the 4.75 m long tidal flat using idealized surrogate vegetation fixed to the plywood. During the study, several different marshes with different plant characteristics could be modelled in each flume by



meadows of *S. alterniflora* stems were simulated in the experiments using a reduced number of oversized cylinders. The stem densities of these scaled meadows were $N_v = 125, 295,$ and 450 stems/m^2 , representing meadows with low-, medium-, and high-densities, equivalent to $150, 350,$ and 550 stems/m^2 of live vegetation (see **Figure 4**). Two stem heights, $h_v = 0.090$ and 0.025 m were investigated in the experiments, representing *S. alterniflora* meadow heights of 1.8 and 0.5 m respectively, nominally representing two different periods of the growth season.

4.3 Dyke Design and Construction

The performance of four different dyke designs located at the leeward end of the model test flumes was examined in these experiments (see **Figure 5**). The first design was considered typical for dykes throughout Atlantic Canada and featured an impermeable dyke core with two layers of riprap on the seaside only (herein referred to as a simply reinforced dyke). Three additional designs, representing various potential methods for upgrading the simply reinforced dyke, were also studied. The second design (armoured dyke) was created by adding two layers of riprap on the crest and leeside of the structure while maintaining the same crest elevation. The third design

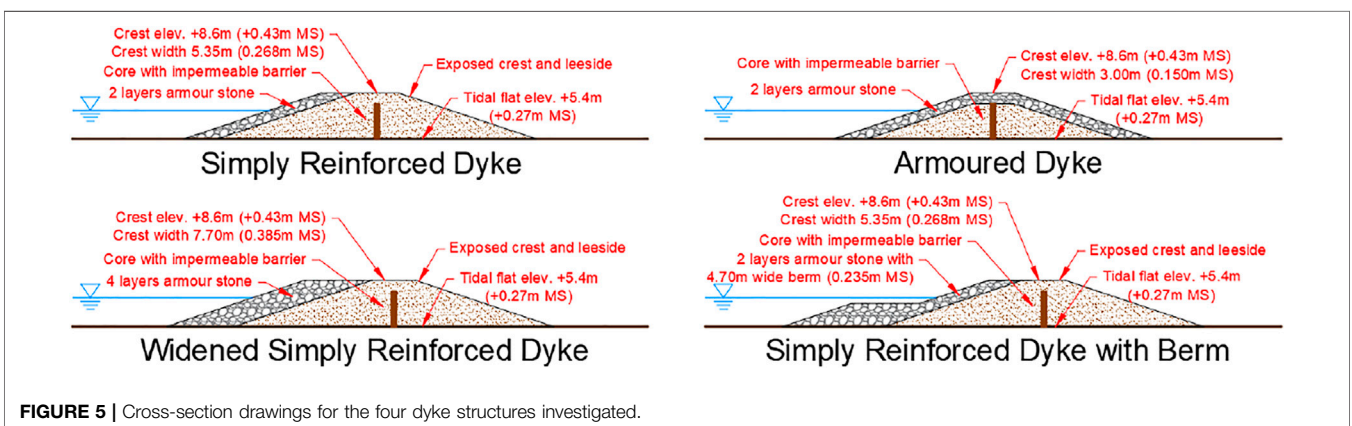
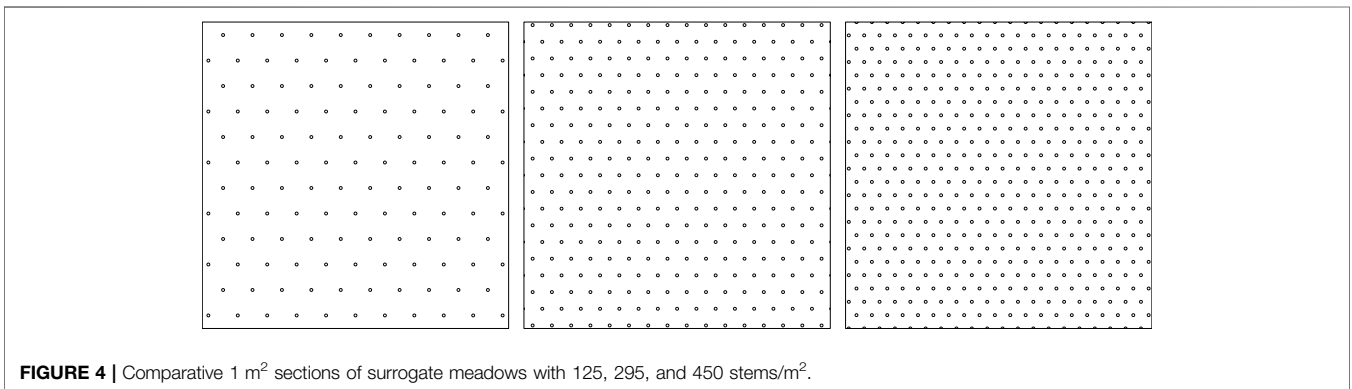


TABLE 2 | Experiment setup for Test Series 1–5.

Test series	Flume	Structure type	Marsh width, L_v (m)	Vegetation density, N_v (stems/m ²)	Vegetation height, h_v (m)	Vegetation type
TS1 41 ^a	1	Armoured dyke	4.75 (95)	0	0	No Veg Rigid
	2			125	0.090 (1.8)	
	3			295		
	4			450		
TS2 17 ^a	1	Gravel beach	4.75 (95)	0	0	No Veg Rigid
	2			125	0.090 (1.8)	
	3			295		
	4			450		
TS3 21 ^a	1	Armoured dyke	4.75 (95)	295	0.090 (1.8)	Rigid
	2	Simply reinforced dyke				
	3	Simply reinforced dyke with berm				
	4	Widened simply reinforced dyke				
TS4 31 ^a	1	Armoured dyke	0	0	0	No Veg Rigid
	2		2.30 (46)	295	0.090 (1.8)	
	3	Simply reinforced dyke with berm	4.75 (95)		0.025 (0.5)	
	4	Armoured dyke		125	0.090 (1.8)	
TS5 31 ^a	1	Armoured dyke	2.30 (46)	0	0	No Veg Rigid
	2			450	0.090 (1.8)	
	3	Simply reinforced dyke with berm		295	0.025 (0.5)	
	4	Widened simply reinforced dyke		4.75 (95)	125	

^aIndicates the number of wave height, wave period, and water level combinations per test series. Values in brackets indicate corresponding full scale values.

(widened reinforced dyke) was created by doubling the thickness of the seaside armour layer. The fourth design (simply reinforced dyke with berm) was created by adding a berm of armour stone on the seaside that was half the height of the structure and four armour stones in thickness. All four model dyke designs featured a crest elevation of +0.43 m (corresponding to +8.6 m above mean sea level at full scale), a typical crest elevation of older dykes in the Tantramar area (Lieske and Bornemann, 2012).

Each model dyke was constructed using carefully prepared stone materials and construction methods. The dyke cores were constructed using a fine gravel with low permeability, but also included impermeable wooden barriers which prevented water from seeping through the dykes into the inland areas. Furthermore, a thin, flexible plastic membrane was placed between the core and armour materials to prevent water from flowing into the core. This method of construction allowed overtopping flows to pass through or above the armour stone on the dyke crest as would occur in the prototype situation. The landward end of each test flume was sealed off so that the water level behind each model structure could be kept lower (using submersible pumps), thereby simulating the situation where the inland area behind the dyke structure is not flooded, which is expected to be the most critical condition for rear slope stability.

The sizing of armour stone was based on Hudson formula calculations and also informed by Nova Scotia Department of Transportation Guidelines. The required armour stone mass M_{50} was calculated as 136 kg at full scale. The armour stone was assumed to have a wide gradation such that $M_{15} = M_{50}/2$ and $M_{85} = M_{50} \times 2$. The corresponding values of M_{15} , M_{50} , and M_{85}

at model scale, accounting for the density difference between the freshwater used in the model and the seawater in prototype, were 7.5, 15.1, and 30.2 g. Model stone materials were prepared to closely replicate the gradation and characteristics of the prototype material. During construction of the various dyke structures, due care was taken to ensure that stones with aspect ratios greater than 3:1 were not used (i.e., stones where either the length, width or height was more than three times larger than any other dimensions). This was important since flatter stones are more likely to move or overturn under wave action.

4.4 Test Conditions and Instrumentation

Particulars of the marsh-dyke system in each test flume during each test series are given in **Table 2**. Each setup was chosen in order to obtain results needed to independently assess the influence of key variables including: vegetation density, vegetation (stem) height, cross-shore marsh width, type of vegetation (rigid or flexible), and dyke structure type. For Test Series 2, the dyke structures were replaced with gently sloping gravel beaches featuring less than 5% wave reflectance, so that wave conditions across the artificial marshes could be measured with minimal influence of reflected waves. Hence, much of the analysis concerning wave attenuation presented in the following Section is based on data gathered during Test Series 2.

The wave conditions and water levels selected for testing were generally representative of conditions along the Canadian Atlantic coast where marsh-dyke systems exist (see **Table 3**), with a particular focus on storm conditions (higher water levels and energetic waves) that could overtop and/or damage the

TABLE 3 | Range of irregular wave parameters.

Water depth at tidal flat, d (m)	Significant Wave Height, H_{m0} (m)	Peak wave period, T_p (s)	Keulegan-Carpenter #	Reynolds #
0.05 (1.0)	0.05 (1.0)	0.67, 1.34, 2.01, 2.68 (3, 6, 9, 12)	12–152 (243–3,044)	1,133–3,553 (5,067–15,889)
	0.075 (1.5)	1.34, 2.01, 2.68 (6, 9, 12)		
	0.10 (2.0)	1.34, 2.01, 2.68 (6, 9, 12)		
0.075 (1.5)	0.05 (1.0)	0.67, 1.34, 2.01, 2.68 (3, 6, 9, 12)	13–212 (268–4,248)	1,249–4,959 (5,587–22,176)
	0.075 (1.5)	1.34, 2.01, 2.68 (6, 9, 12)		
	0.10 (2.0)	1.34, 2.01, 2.68 (6, 9, 12)		
0.10 (2.0)	0.05 (1.0)	0.67, 1.34, 2.01, 2.68 (3, 6, 9, 12)	14–173 (273–3,464)	1,273–4,432 (5,694–19,821)
	0.075 (1.5)	1.34, 2.01, 2.68 (6, 9, 12)		
	0.10 (2.0)	1.34, 2.01, 2.68 (6, 9, 12)		
0.12 (2.4)	0.05 (1.0)	0.67, 1.34, 2.01, 2.68 (3, 6, 9, 12)	12–168 (241–5,359)	1,124–5,170 (5,026–23,121)
	0.075 (1.5)	1.34, 2.01, 2.68, 3.35 (6, 9, 12, 15)		
	0.10 (2.0)	1.34, 2.01, 2.68 (6, 9, 12)		
	0.15 (3.0)	1.34, 2.01, 2.68, 3.35 (6, 9, 12, 15)		

(Values in brackets indicate corresponding full scale values).

dykes. **Table 2** specifies the number of wave height, wave period, and water level combinations investigated in each test series. Overall, the testing program consisted of 141 unique tests.

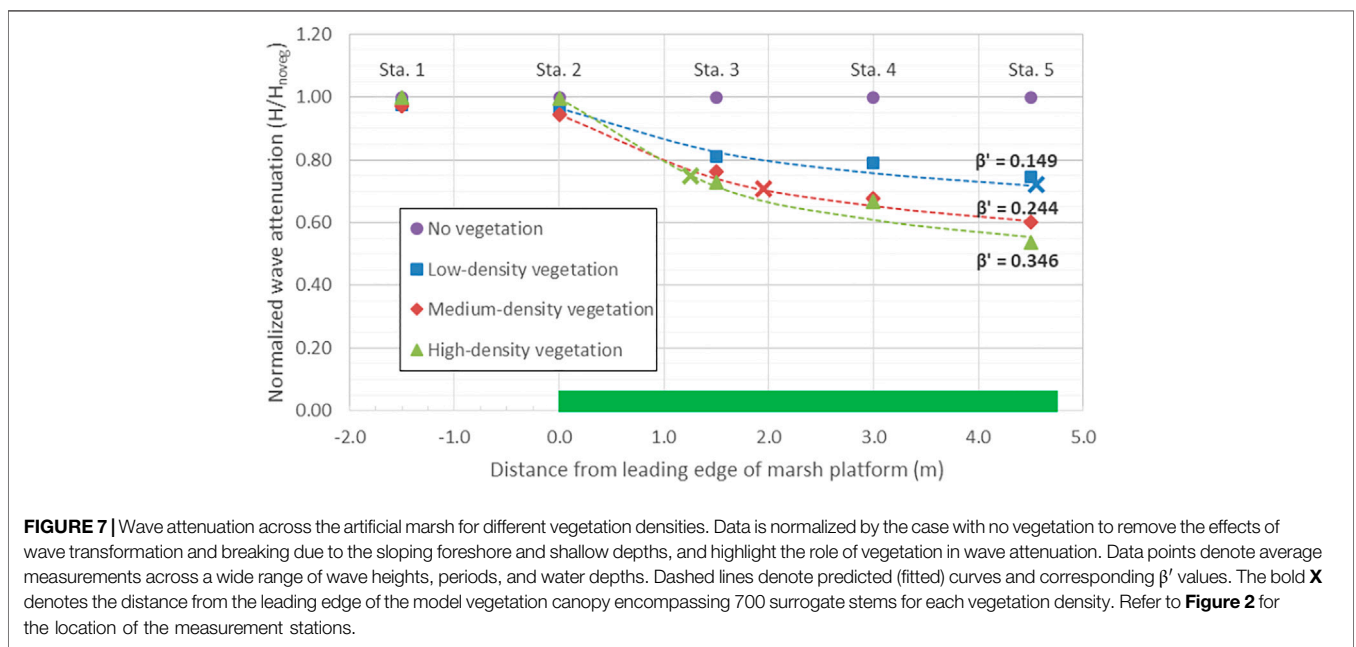
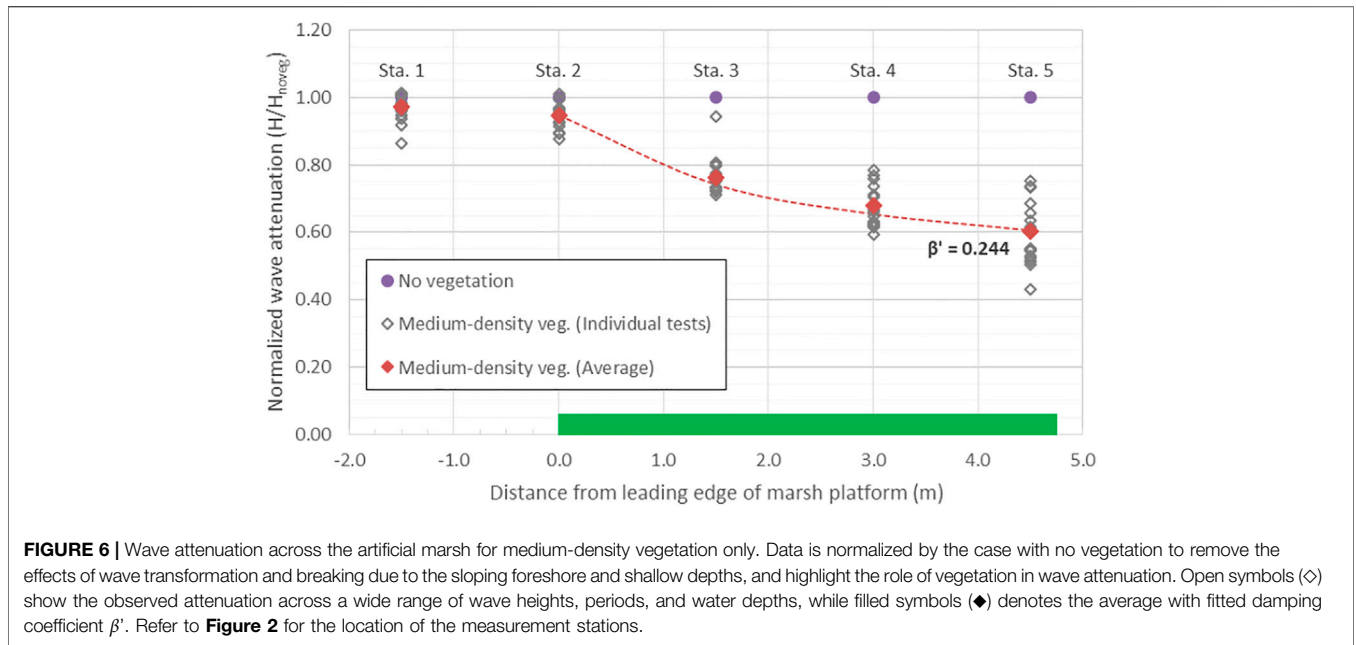
The wave signals for tests with irregular waves were synthesized from a family of JONSWAP-type spectra with a 3.3 peak enhancement factor approaching from a single direction. However, due to the shallow water conditions in the CWB and the natural growth of sub- and super-harmonics, the spectral shapes, and the distribution of energy with frequency in the experiments were typical of shallow water conditions. The test program included significant wave heights (H_{m0}) ranging from 0.05 to 0.15 m (corresponding to 1.0–3.0 m at full scale) and peak wave periods (T_p) ranging from 0.63 to 3.35 s (corresponding to 3–15 s at full scale). These conditions respect the guidance of Hughes (1993) and Heller (2011) for minimizing scale effects on wave propagation caused by surface tension. Water depths on the tidal flat ranged from 0.05 to 0.12 m (corresponding to 1.0–2.4 m at full scale). Each wave signal featured a non-repeating sequence of approximately 1,000 irregular waves, thus the duration of each wave signal and test varied depending on the peak wave period, ranging from ~10.9 to 38.9 min long (corresponding to ~0.8–2.9 h at full scale). One-thousand waves was selected to ensure that each signal included a statistically representative distribution of larger wave heights and crest elevations, since wave overtopping and armour stone stability are typically sensitive to the few largest waves in a sea state. Water levels were adjusted in the model by filling or draining the basin until the desired level was reached.

Twenty-two capacitance-type probes were used to measure water surface displacement at several locations of interest in each test flume. Two probes were located in deeper water near the wave generator to measure offshore wave conditions, while the others were positioned such that five probes were deployed inside each flume as shown in **Figure 2** (one above the sloping foreshore and the other four distributed across the artificial marsh). The probes

were configured to record water levels at a sampling frequency of 50 Hz and were (re)calibrated before each test series by changing their elevation with respect to a fixed (known) water level. The wave probes featured a highly linear and stable response, with calibration errors typically less than 0.5% over their calibration range. Comprehensive time-domain and frequency-domain analysis algorithms were applied to analyze the wave conditions measured in the model in detail.

Four simple, accurate and reliable overtopping measurement systems were deployed, one in each test flume. Each overtopping measurement system consisted of a collection tray positioned to collect water passing over the dyke crest and convey it to a water storage reservoir fitted with a capacitance water level gauge located on the leeside of the dyke. Wave overtopping was quantified as a volumetric flow rate per unit width passing over the top of the dyke crest. This overtopping measurement system was best suited for measuring moderate-to-heavy overtopping flows (e.g., greater than 1 L/s/m at full scale); measuring smaller volumes of splash and spray was less precise. The overtopping collection trays were positioned at the rear slope break of the dyke crest atop nominally two layers of armour stone. Small overtopping events in which the wave runup reached the crest elevation, generating overtopping flows through the armour stone on the dyke crest, were not captured by the overtopping measurement system. It is noted that typical dykes have a drainage ditch along their leeside which can handle some degree of overtopping flow. Only larger overtopping events featuring green water flowing over the crest and reaching the rear slope break were captured by the overtopping measurement systems in these experiments.

A photographic damage analysis system comprising four remotely-operated digital cameras was used to monitor the stability of the armour stones on each of the four dyke structures. Since each camera remained fixed throughout a test series, by comparing photographs taken before and after each test segment, damage could be assessed and quantified based on the number of individual stones that were displaced during each test



segment. The effect of marsh vegetation on armour stone stability will be discussed briefly in the next section.

5 RESULTS AND DISCUSSION

5.1 Effect of Vegetation Density

Previous research has identified a strong correlation between vegetation density and wave damping, and this correlation was further confirmed in these experiments. Not only did the rate of

wave attenuation increase with increasing vegetation density, but the amount of wave overtopping recorded at the dyke, and the damage to the dyke itself was reduced as well. **Figure 6** shows relative wave heights (wave height with vegetation normalized by corresponding wave height without vegetation) measured across the tidal flat comprised of medium-density vegetation for a range of wave conditions and water levels. Measurement locations are shown in **Figure 2**. This normalization of wave height is necessary to isolate the effects of vegetation, since the wave conditions across the artificial marshes in these experiments were generally

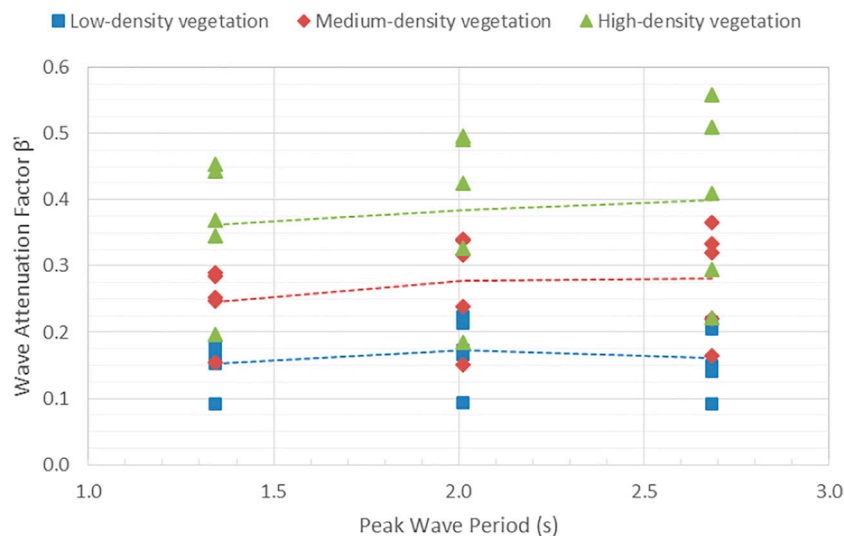


FIGURE 8 | Variation in wave attenuation factor β' with wave peak period for artificial marshes with different vegetation densities. Symbols denote results from individual tests spanning a range of wave heights and water depths. Dashed lines connect average β' values at each wave period.

strongly influenced by the effects of shoaling and depth-limited wave breaking, and, to a lesser extent, flume friction effects (Maza et al., 2019). For test flumes with vegetation, measured significant wave heights at each probe were normalized by H_{m0} values measured at corresponding locations in the flume with no vegetation (i.e., Flume 1 in Test Series 2; refer to **Table 2**). **Figure 6** shows the spread of observed wave attenuation for individual tests spanning a broad range of significant wave heights, peak wave periods, and water depths. For each test, the damping coefficient β' (Eq. 3) was evaluated by least squares regression to the significant wave heights measured across the model marsh canopy. Values from individual tests were averaged to permit comparison across different vegetation densities (discussed below).

Similarly, **Figure 7** shows relative wave heights (wave height with vegetation normalized by corresponding wave height without vegetation) measured across the tidal flat as a function of vegetation density. Average β' values (derived by averaging results from multiple tests with different wave conditions and water depths) for the three different artificial marshes considered in these experiments are shown in **Figure 7**. Although different plant species were investigated by Maza et al. (2015), the β' values derived from the present experiments (0.149–0.346) are similar to those observed by Maza et al. at lower water depths (0.124–0.286), which involved submergence ratios similar to the present study (1.0 in Maza et al. compared to an average of 0.92 in the present experiments).

As shown in **Figure 7**, significant wave heights in the low-density, medium-density and high-density vegetation were 28, 40 and 46% lower (respectively) than those in the flume with no vegetation for the same test conditions. Therefore, higher vegetation density does lead to increased wave attenuation, as expected, but there appears to be a diminishing return on

additional bio-mass leading to additional wave attenuation, at least for the range of densities tested in this study.

Looking at the data points along each individual curve in **Figure 7**, the majority of the wave damping occurs in the first third of the marsh (i.e., between Stations 2 and 3). Averaging over the full range of water level and sea state conditions investigated, there was a 19% reduction in significant wave height across the first 1.5 m of the low-density marsh, compared to a further 9% reduction across the following 3.25 m of marsh. For the high-density marsh, there was a 27% reduction across the first 1.5 m long section versus a further 19% reduction across the remainder.

Stakeholders looking to make use of vegetated tidal flats to augment shore protection should consider creating expansive marshes wherever possible, not only from a wave attenuation and flood risk reduction perspective but also for the environmental co-benefits they bring. Where expansive marshes are not possible, this data suggests that denser vegetation is preferred from a wave attenuation perspective, as opposed to sparser vegetation. **Figure 7** shows that narrower denser marshes can be considered roughly equivalent to wider marshes with sparser vegetation. For example, 700 dowels placed in the low-density configuration (denoted by the blue X in **Figure 7**) spans $X = 4.55$ m and yields ~28% wave attenuation on average. However, 700 dowels placed in the medium-density configuration (denoted by the red X) occupies $X = 1.95$ m of horizontal distance and yields ~29% attenuation on average across a broad range of wave conditions and water depths, while the same number of dowels in the high-density configuration (denoted by the green X) spans $X = 1.25$ m and yields ~25% attenuation on average.

Figure 8 shows the observed variation in wave attenuation factor β' with peak wave period based on the present experiments. In this figure, symbols denote results for individual tests and dashed lines connect average wave attenuation factors for each wave period. For the range of conditions investigated in these

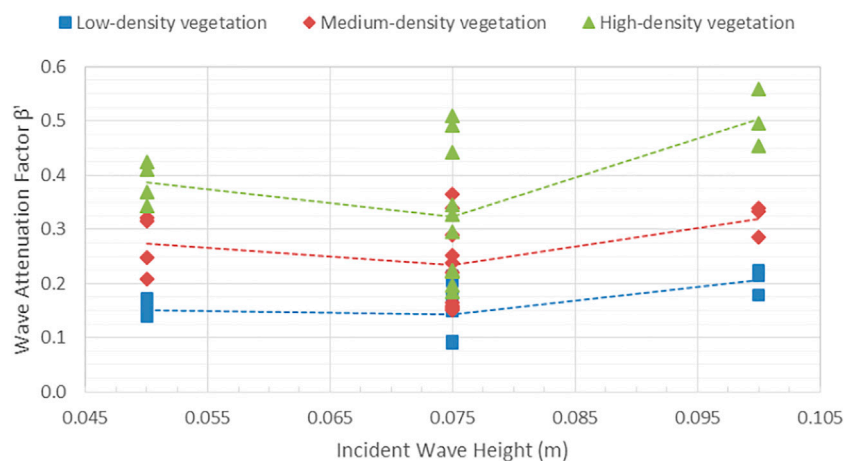


FIGURE 9 | Variation in wave attenuation factor β' with significant wave height for artificial marshes with different vegetation densities. Symbols denote results from individual tests spanning a range of wave periods and water depths. Dashed lines connect average β' values for each significant wave height.

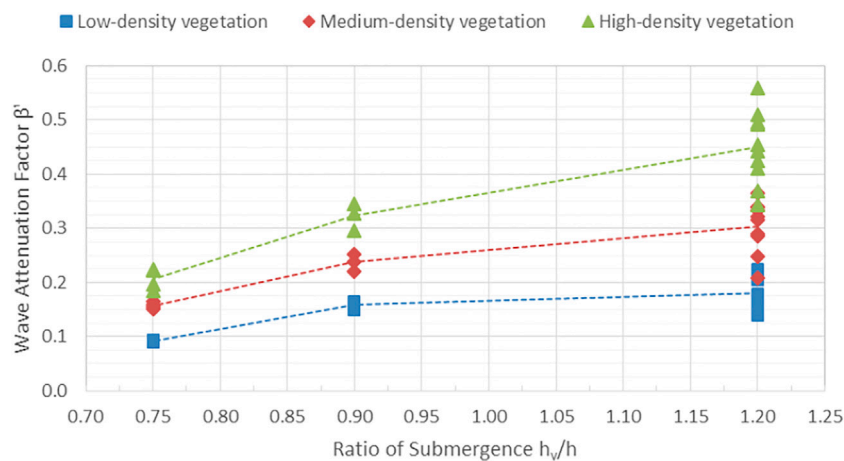


FIGURE 10 | Variation in wave attenuation factor with submergence ratio for artificial marshes with different vegetation densities. Symbols denote results from individual tests spanning a range of wave conditions. Dashed lines connect average values for each submergence ratio.

tests, no clear dependence of attenuation factor on wave period was identified. While some wave period dependency was identified for specific test conditions (particular combinations of water depth and wave height), the trend was not consistent across all test conditions.

Contrary to the findings of Wu and Cox (2015b), no significant correlation between wave steepness and wave attenuation was observed across the range of conditions investigated in this study.

Based on a study by Maza et al. (2019), damping coefficients determined for various water depths, wave heights and wave periods indicated that, in general, higher damping coefficients are associated with higher wave heights and shorter wave lengths (i.e., smaller wave periods). In addition, higher correlations were found between the damping coefficient and

wave height than with wave steepness, indicating that wave height has greater control than wave period in terms of attenuation capacity.

Figure 9 shows the variation in wave attenuation factor (β') with incident wave height based on data from Test Series 2, where the dykes in each flume were replaced by absorbing gravel beaches with low wave reflectance. The results show that wave attenuation is, on average, greatest (largest β') for the highest incident waves investigated in this study, which is consistent with the results of Maza et al. (2019). However, further analysis (presented and discussed below) makes it clear that submergence ratio plays a more significant role and helps to explain the degree of scatter seen in **Figure 9**. Analysis to detect correlations between wave attenuation factor and wave steepness were undertaken, but no clear trends were evident for the range of conditions in Test Series 2.

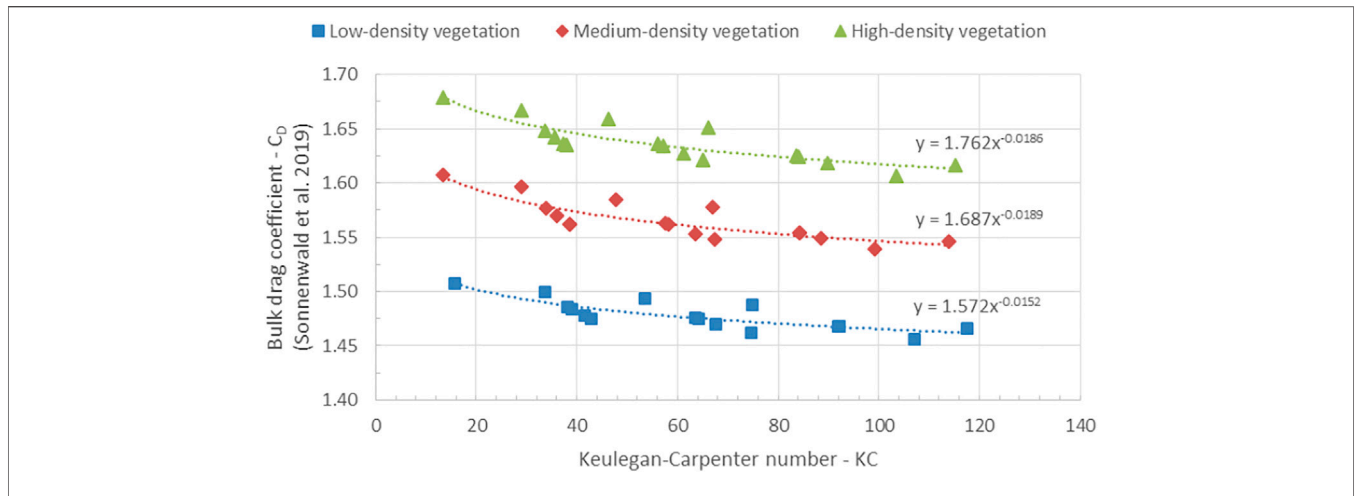


FIGURE 11 | Bulk drag coefficient versus Keulegan-Carpenter number for artificial marshes with low, medium, and high vegetation densities.

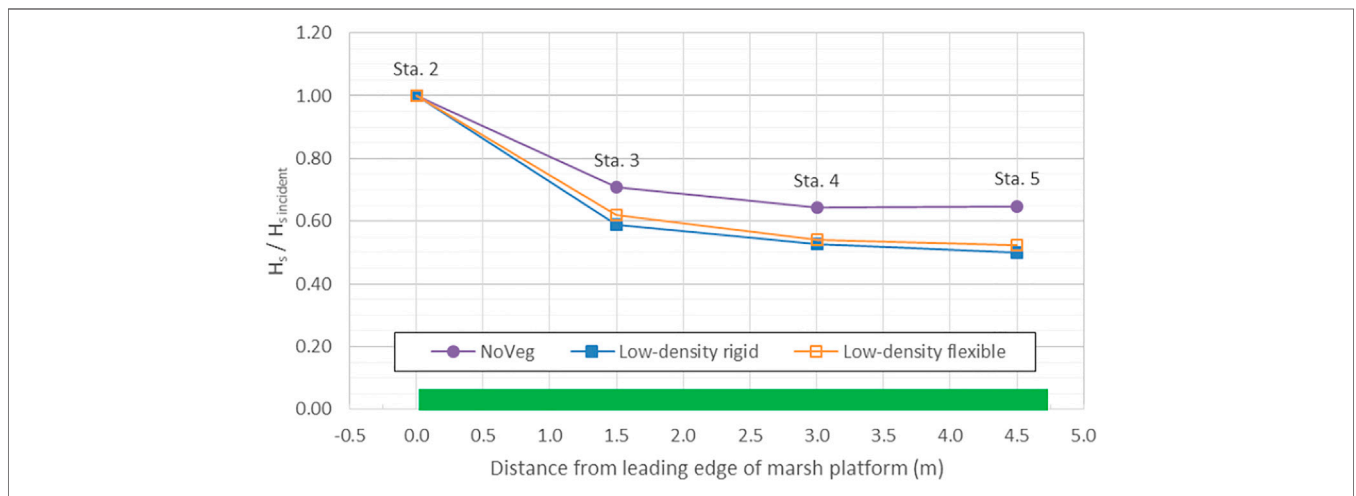


FIGURE 12 | Wave attenuation across similar artificial marshes comprised of rigid and flexible vegetation. Data is normalized by the incident wave height at the edge of the marsh (@ Station 2). Note that this figure includes wave height attenuation due to depth-limited breaking.

The relationship between wave attenuation factor (β) and the ratio of submergence derived from the present experiments is presented in **Figure 10**, where symbols denote results from individual tests spanning a range of wave conditions, while dashed lines connect average values for each submergence ratio. As seen in many previous studies, wave attenuation clearly increases as plant height (submergence) increases relative to the local water depth. Although results for only three submergence ratios are available from this dataset, the data suggests that the rate of increase with submergence ratio is greater for submergence ratios less than 0.9, decreasing as the vegetation becomes emergent in still water.

Using data from Test Series 2, the bulk drag coefficient, C_D , was calculated according to the formula proposed by Sonnenwald et al. (2019), see **Eq. 7**. **Figure 11** shows the resulting relationship between the bulk drag coefficient and the

KC number defined in **Eq. 6**. These results suggest that for larger KC number ($KC > 80$), the low-, medium-, and high-density marshes studied in these experiments are associated with bulk drag coefficients of approximately 1.47, 1.55, and 1.63, respectively, and that bulk drag coefficients for all three marshes increase gradually as KC number decreases towards $KC \sim 10$. These results are generally consistent with the findings of Ozeren et al. (2014), who found that C_D was dependent on KC when $KC < 10$. In these experiments, $12 < KC < 268$, suggesting all were in the range where drag forces dominate and the drag coefficient is weakly dependent on KC . At field (full) scale, $268 < KC < 2,351$ would be typical for the same range of wave and water level conditions, assuming stem diameters of 9.5 mm, and therefore bulk drag coefficients observed in the present experiments are expected to slightly over-predict field conditions.

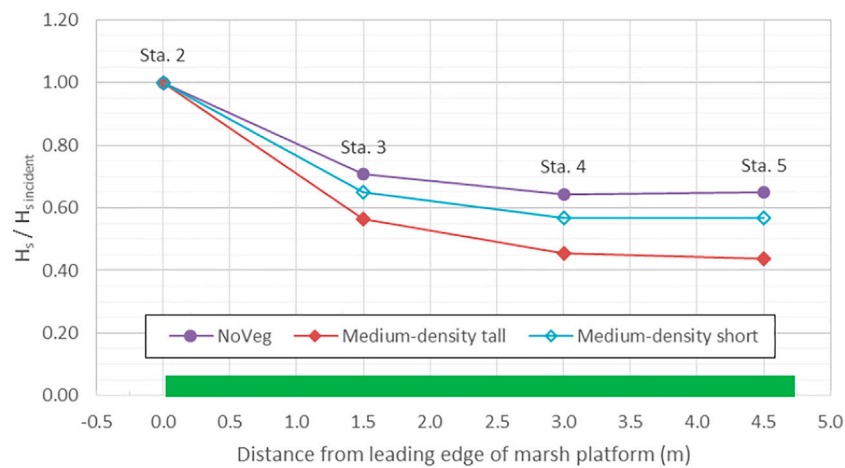


FIGURE 13 | Wave attenuation across similar artificial marshes featuring different vegetation heights. Data is normalized by the incident wave height at the edge of the marsh (@ Station 2). Note that this figure includes the effect of wave transformation and breaking due to the sloping foreshore.

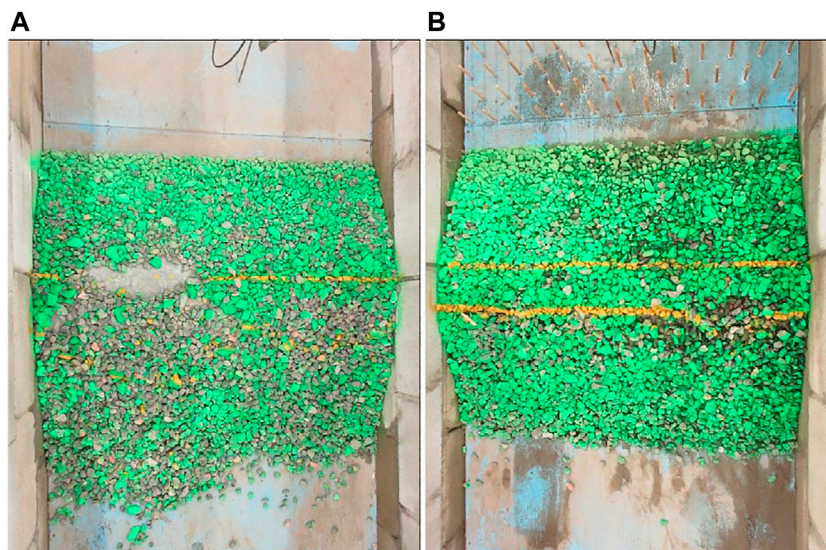


FIGURE 14 | Comparison of damage to identical dykes built behind a salt marsh platform; without vegetation (A) and with vegetation (B). Waves approached from the top in these images.

5.2 Effect of Vegetation Flexibility and Submergence

Test Series 4 was conducted to investigate the effects of vegetation height (or submergence ratio) and stem flexibility on the resulting wave attenuation. **Figure 12** compares wave attenuation across the model marsh for otherwise identical marshes comprised of rigid and flexible vegetation. In this figure, the wave height attenuation across the marsh platform for the no vegetation (NoVeg) case is primarily due to depth-limited wave breaking. Across the wide range of significant wave heights, peak wave periods and water depths investigated, the additional wave attenuation due to flexible vegetation is roughly 90% of the additional attenuation due to comparable rigid vegetation.

Although plant stiffness was not the main focus of these tests, and plant flexibility was not modelled with strict parametric specificity, these results are consistent with the findings of Maza et al. (2015), where increased plant rigidity was shown to correlate with increased wave attenuation.

The influence of plant submergence ratio on wave height attenuation is plotted in **Figure 10** and discussed briefly in the previous section, where it is shown that wave attenuation capacity increases with increasing submergence ratio. In a similar vein, **Figure 13** shows the effect of plant submergence (or height) on wave attenuation across otherwise similar model marshes. As in **Figure 12**, the wave height attenuation curves in this figure are based on averaging results from several tests with different wave

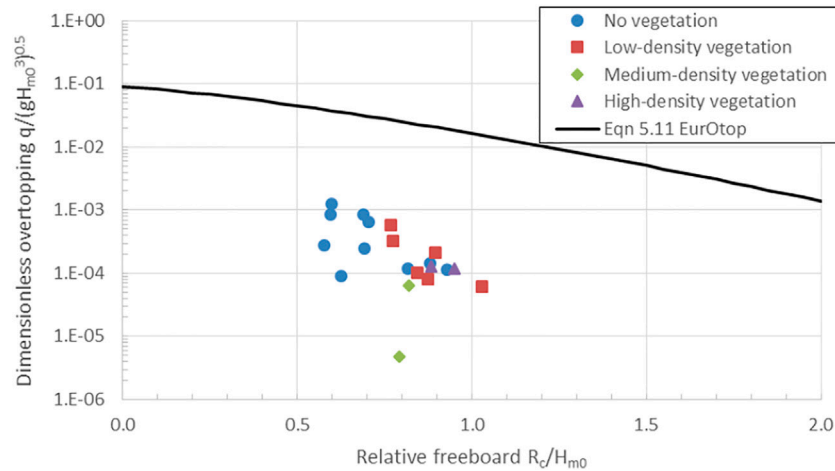


FIGURE 15 | Wave overtopping at four identical dykes for different vegetation densities.

conditions, and include the effects of depth-limited wave breaking. Stems in the tall marsh were simulated using 0.09 m tall rigid dowels, whereas 0.025 m tall dowels were used in the short marsh (28% of the tall plant height). **Figure 13** shows that the additional wave height attenuation due to the short stems (relative to the NoVeg case) was roughly $1/3^{\text{rd}}$ of the additional attenuation due to the taller ones. These results are consistent with the results shown in **Figure 10** and the findings by other authors (Arkema et al., 2013; Anderson and Smith, 2014) who investigated the effect of water depth on wave attenuation capacity and found a significant influence on wave height decay, specifically that emergent conditions led to higher amounts of wave attenuation. Wave attenuation due to shorter, broken stems is an important topic, particularly for higher latitude regions where marsh plants tend to die off following the summer growing season, thus reducing their capacity to dissipate wave energy and limit flood risk.

5.3 Effect of Vegetation on Dyke Performance

The presence (or absence) of vegetation was a strong function of dyke performance. **Figure 14** shows a comparison of two identical dykes built in the lee of salt marsh platforms subject to the same series of increasingly harsh sea states and water levels. At the end of the test series, the dyke without protective vegetation (shown on the left) suffered significant damage, exposing the core at the seaside crest and causing significant scouring on the leeside. In stark contrast, the dyke fronted by a 4.75 m length of low-density marsh (shown on the right) sustained only minor damage to the leeside crest. Identical dykes protected by medium-density and high-density marshes (not pictured) showed effectively no damage following exposure to identical test conditions. **Figure 15** shows a comparison of the overtopping measured at four identical dykes fronted by varying vegetation fields. Out of the 41 sea states examined in Test Series 1, the dykes typically only experienced overtopping as a result of

the largest wave heights in combination with extreme water levels. From **Figure 15**, it is clear that the NoVeg case not only saw overtopping in a greater number of these sea states, but that the overtopping volumes were also significantly larger. It is noted that these overtopping results are notably smaller than predicted by Equation 5.11 from EurOtop (Van der Meer et al., 2018), however this formula likely does not consider a dyke fronted by a long tidal flat. These results emphasize the potential effectiveness of coastal salt marshes in dissipating wave energy, lessening overtopping and reducing damage of adjacent coastal infrastructure in storm conditions, provided that the marsh itself is able to survive the storm without being damaged.

5.4 Effect of Dyke Structure Design

A detailed investigation of wave overtopping and damage to the dyke structures was not the primary focus of this study; however, some general commentary based on observations made during the testing program is presented herein. Four different dyke structure designs (see **Figure 5**) were modelled and investigated in Test Series 3 with identical foreshore marshes to help inform decisions concerning potential upgrading of older dyke structures. Analysis of the wave data measured on the tidal flats suggests that the level of wave reflection was similar in each flume, and that the degree of wave attenuation across the model marsh was also similar in each flume.

However, clear differences in overtopping flowrates (and damage) were measured in each flume, depending on the dyke design (see **Figure 16**). The armoured dyke (requiring a rock armour volume of 15.4 m^3 per linear metre of full-scale structure), will be considered as a base case for comparison. The mean overtopping discharge for the armoured dyke, averaged across a broad range of test conditions, was 1 L/s/m . Despite this overtopping, the armour on the leeside crest and slope sustained negligible damage. In comparison, the simply reinforced dyke, with a slightly wider crest but requiring only $7.5 \text{ m}^3/\text{m}$ of rock armouring, saw a 36% reduction in overtopping discharge. However the unprotected leeside crest and slope saw

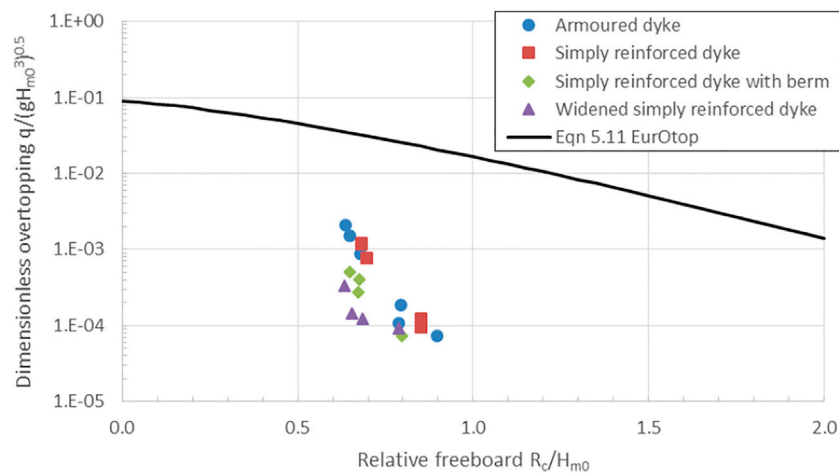


FIGURE 16 | Wave overtopping at four different dyke structures with identical marsh platforms.

comparatively greater damage, though not serious enough to jeopardize the overall integrity of the dyke.

In comparison, significantly fewer overtopping events and smaller flowrates were measured at the simply reinforced dyke with berm and the widened simply reinforced dyke (74 and 86% reductions in mean overtopping discharge, respectively). Each of these dyke designs requires 15.0 m^3 of armour stone per linear metre of structure. The berm was observed to trigger earlier wave breaking, and the additional volume of porous rock in the widened dyke was effective at reducing run-up and overtopping. In both cases, despite the lower overtopping volumes, damage to the leeside crest and slope was similar to that observed on the simply reinforced dyke (without berm), which may point to the high mobility of the impermeable core material under the conditions tested. Overall, the widened simply reinforced dyke was most effective in reducing mean overtopping discharge, however the armoured dyke provided the best protection in terms of leeside stability.

In all four cases, the seaside armouring saw only minor damage, in the form of rocking and/or small displacements. It should be noted that all four dykes saw effectively zero overtopping (or damage to the leeside) in all but the most energetic test conditions featuring the highest water levels combined with the largest wave heights. These results provide information on the relative ability of the upgraded structures to reduce overtopping and limit damage in extreme conditions. The relative benefits of each potential dyke upgrade must be balanced against the relative cost of implementation, which can be assumed to be roughly proportional to the volume of armour stone required.

6 CONCLUSION

A series of scaled laboratory experiments were conducted to investigate the function of coastal salt marshes as part of a coastal marsh and dyke system, and to determine the effectiveness of

marsh vegetation in dissipating wave energy and reducing wave overtopping and damage under a broad range of wave and water level conditions, including harsh conditions, representative of Canadian coastal regions. A secondary goal was to assess the feasibility and efficacy of using simple, low-cost scale model surrogates to represent salt marsh vegetation in scale model testing. The model dyke and marsh platform features investigated in this study were based on archetypes found in Atlantic Canada, in particular the Tantramar Marsh on the Chignecto Isthmus between New Brunswick and Nova Scotia where *Spartina alterniflora* (smooth cordgrass) dominates.

This study addressed several of the research knowledge gaps highlighted by Markov (2021). In particular, two different plant heights were investigated as a proxy to the seasonal variation in marsh plant posture and stature typical of higher latitude regions, and tests were conducted across a much broader range of wave heights, periods, and water levels than previously seen in full scale (or near full scale) experiments using live or surrogate vegetation.

This research confirmed the benefit of tidal flats hosting coastal marshes for attenuating waves, reducing overtopping volumes and lessening damage to dyke structures. As expected, taller and denser marshes were more effective in attenuating wave energy for a given marsh width. From a wave attenuation perspective, the study results show that narrow, densely vegetated marshes (i.e., 25 m wide marsh with $\sim 450 \text{ stems/m}^2$) provide similar wave attenuation capacity as wider marshes with sparser vegetation (i.e., $\sim 90 \text{ m}$ wide marsh with $\sim 150 \text{ stems/m}^2$). Of course, stakeholders looking to make use of vegetated tidal flats to augment shore protection should consider creating expansive marshes wherever possible, not only from a wave attenuation perspective but also for the ancillary environmental co-benefits they bring.

This study is certainly limited by the use of artificial plants to represent coastal marshes. As noted by Tinoco et al. (2019), several authors have shown that simplifications in experimental setup, such as the use of rigid elements, a single stem diameter, a single element height, and a regular or staggered layout, can bias study outcomes, by

either hiding or amplifying some of the relevant physical processes found in natural conditions. However, representing coastal marshes in a simple manner at reduced scale made it possible to study wave interaction with entire marsh-dyke systems in controlled laboratory conditions, efficiently study the effect of numerous changes in marsh properties and dyke characteristics, and study relatively high-energy wave conditions; investigations that would be impractical or highly demanding and expensive using live plants at full scale. Despite its limitations, it is believed that the present study contributes useful new information leading to greater understanding of the behaviour of marsh-dyke systems, the wave attenuation over wide marshes in a broad range of depths and wave conditions, and the sensitivity of these processes to various marsh characteristics and properties, such as plant density, plant height (submergence), stem flexibility and marsh width. Moreover, results from the present study can be used to inform the representation of coastal marshes in physical and numerical models.

It is noted that Webb et al. (2018) highlighted that *S. alterniflora* marsh vegetation in southern Alabama was stable when significant wave heights are less than 0.2 m 80 percent of the time and less than 0.3 m 95 percent of the time. In comparison, some of the wave heights investigated in this study were considerably larger (up to $H_s = 3$ m at full scale) and may have been sufficient to cause erosion and/or damage in natural settings. In reality, it is likely that at least the seaward edge of the marsh may have experienced some erosion as a result of these energetic conditions, though conceivably some sort of soil stabilization measures could be applied to reduce erosion in vulnerable areas. When reviewing the results of this study and assessing the performance and efficacy of salt marshes, it is important to consider the potential for soil erosion, plant damage and loss of wave attenuation capacity in high-energy conditions, although these processes were not included in the present study.

Although several researchers have conducted experiments with live plants in test facilities, further research is required to better understand wave attenuation caused by vegetation. Topics where further research is needed include examining wave attenuation capacity over the plant life cycle (spring growth, summer, and winter dormancy periods), understanding erosion and plant damage processes in high-energy wave conditions, and

understanding how to best protect and establish young plants early in their life cycle or in more exposed locations. Additional research, especially in connection with field studies, is recommended and encouraged. Future work by the authors will focus on extending the analysis of the data obtained in the current study (particularly with respect to overtopping and stability of the dyke structures), developing and validating improved approaches for representing other types of coastal vegetation in scale model studies and investigating the behaviour and performance of other types of nature-based coastal infrastructure.

DATA AVAILABILITY STATEMENT

The raw data supporting the conclusions of this article will be made available by the authors, without undue reservation.

AUTHOR CONTRIBUTIONS

SB designed and led the experiments described in the paper and is the primary author of this paper. EM, AC, and PK acted in an advisory role before and during the experiments, and are secondary authors of this paper.

FUNDING

This research was supported by the Climate-Resilient Buildings and Core Public Infrastructure Initiative through Infrastructure Canada and by the Nature-Based Infrastructure for Coastal Resilience and Risk Reduction project through the Canadian Safety and Security Program (CSSP-2019-CP-2444).

ACKNOWLEDGMENTS

The NRC-OCRE technical staff, in particular Alistair Rayner, are recognized for their efforts in model construction and testing.

REFERENCES

- Anderson, M. E., and Smith, J. M. (2014). Wave Attenuation by Flexible, Idealized Salt Marsh Vegetation. *Coast. Eng.* 83, 82–92. doi:10.1016/j.coastaleng.2013.10.004
- Arkema, K. K., Guannel, G., Verutes, G., Wood, S. A., Guerry, A., Ruckelshaus, M., et al. (2013). Coastal Habitats Shield People and Property from Sea-Level Rise and Storms. *Nat. Clim. Change* 3 (10), 913–918. doi:10.1038/nclimate1944
- Augustin, L. N., Irish, J. L., and Lynett, P. (2009). Laboratory and Numerical Studies of Wave Damping by Emergent and Near-Emergent Wetland Vegetation. *Coast. Eng.* 56, 332–340. doi:10.1016/j.coastaleng.2008.09.004
- Barbier, E. B., Hacker, S. D., Kennedy, C., Koch, E. W., Stier, A. C., and Silliman, B. R. (2011). The Value of Estuarine and Coastal Ecosystem Services. *Ecol. Monogr.* 81 (2), 169–193. doi:10.1890/10-1510.1
- Barron, S., Canete, G., Carmichael, J., Flanders, D., Pond, E., Sheppard, S., et al. (2012). A Climate Change Adaptation Planning Process for Low-Lying, Communities Vulnerable to Sea Level Rise. *Sustainability* 4 (9), 2176–2208. doi:10.3390/su4092176
- Blackmar, P. J., Cox, D. T., and Wu, W.-C. (2014). Laboratory Observations and Numerical Simulations of Wave Height Attenuation in Heterogeneous Vegetation. *J. Waterw. Port. Coast. Ocean. Eng.* 140 (1), 56–65. doi:10.1061/(asce)ww.1943-5460.0000215
- Bridges T. S., King J. K., Simm J. D., Beck M.W., Collins G., Lodder Q., et al. (Editors) (2021). *International Guidelines on Natural and Nature-Based Features for Flood Risk Management* (Vicksburg, MS: U.S. Army Engineer Research and Development Center).
- Bridges, T. S., Wagner, P. W., Burks-Copes, K. A., Bates, E. M., and Collier, Z. (2014). *Use of Natural and Nature-Based Features (NNBF) for Coastal Resilience*. Vicksburg: U.S. Army Engineer Research and Development Center. Report ERDC SR-15-1.
- Browder, G., Ozment, S., Rehberger Bescos, I., Gartner, T., and Lange, G. M. (2019). *Integrating Green and Gray: Creating Next Generation Infrastructure*. Washington: World Bank and World Resources Institute. <https://openknowledge.worldbank.org/handle/10986/31430>.
- Bush, E., and Lemmen, D. S. (2019). *Canada's Changing Climate Report*. Ottawa: Government of Canada.

- Costanza, R., Pérez-Maqueo, O., Martinez, M. L., Sutton, P., Anderson, S. J., and Mulder, K. (2008). The Value of Coastal Wetlands for Hurricane Protection. *AMBIO A J. Hum. Environ.* 37 (4), 241–248. doi:10.1579/0044-7447(2008)37[241:tvocwf]2.0.co;2
- Council of Canadian Academies (2019). *Canada's Top Climate Change Risks: the Expert Panel on Climate Change Risks and Adaptation Potential*. Ottawa: Council of Canadian Academies.
- Cranford, P. J., Gordon, D. C., and Jarvis, C. M. (1989). Measurement of Cordgrass, *Spartina Alterniflora*, Production in a Macrotidal Estuary, Bay of Fundy. *Estuaries* 12 (1), 27–34. doi:10.2307/1351447
- Dalrymple, R. A., Kirby, J. T., and Hwang, P. A. (1984). Wave Diffraction Due to Areas of Energy Dissipation. *J. Waterw. Port. Coast. Ocean Eng.* 110 (1), 67–79. doi:10.1061/(asce)0733-950x(1984)110:1(67)
- Doberstein, B., Fitzgibbons, J., and Mitchell, C. (2019). Protect, Accommodate, Retreat or Avoid (PARA): Canadian Community Options for Flood Disaster Risk Reduction and Flood Resilience. *Nat. Hazards* 98 (1), 31–50. doi:10.1007/s11069-018-3529-z
- Feagin, R. A., Irish, J. L., Möller, I., Williams, A. M., Colón-Rivera, R. J., and Mousavi, M. E. (2011). Short Communication: Engineering Properties of Wetland Plants with Application to Wave Attenuation. *Coast. Eng.* 58, 251–255. doi:10.1016/j.coastaleng.2010.10.003
- Heller, V. (2011). Scale Effects in Physical Hydraulic Engineering Models. *J. Hydraulic Res.* 49 (3), 293–306. doi:10.1080/00221686.2011.578914
- Houser, C., Trimble, S., and Morales, B. (2015). Influence of Blade Flexibility on the Drag Coefficient of Aquatic Vegetation. *Estuaries Coasts* 38, 569–577. doi:10.1007/s12237-014-9840-3
- Hughes, S. (1993). *Physical Models and Laboratory Techniques in Coastal Engineering*. Singapore: World Scientific.
- Jadhav, R. S., Chen, Q., and Smith, J. M. (2013). Spectral Distribution of Wave Energy Dissipation by Salt Marsh Vegetation. *Coast. Eng.* 77, 99–107. doi:10.1016/j.coastaleng.2013.02.013
- Jongman, B. (2018). Effective Adaptation to Rising Flood Risk. *Nat. Commun.* 9 (1), 1986. doi:10.1038/s41467-018-04396-1
- Keimer, K., Schürenkamp, D., Miescke, F., Kosmalla, V., Lojek, O., and Goseberg, N. (2021). Ecohydraulics of Surrogate Salt Marshes for Coastal Protection: Wave–Vegetation Interaction and Related Hydrodynamics on Vegetated Foreshores at Sea Dikes. *J. Waterw. Port. Coast. Ocean Eng.* 147 (6). doi:10.1061/(asce)ww.1943-5460.0000667
- Keulegan, G. H., and Carpenter, L. H. (1958). Forces on Cylinders and Plates in an Oscillating Fluid. *J. Res. Natl. Bur. Stan.* 60 (5), 423–440. doi:10.6028/jres.060.043
- Kirezci, E., Young, I. R., Ranasinghe, R., Muis, S., Nicholls, R. J., Lincke, D., et al. (2020). Projections of Global-Scale Extreme Sea Levels and Resulting Episodic Coastal Flooding over the 21st Century. *Sci. Rep.* 10 (1), 11629. doi:10.1038/s41598-020-67736-6
- Koftis, T., Prinos, P., and Stratigaki, V. (2013). Wave Damping over Artificial *Posidonia Oceanica* Meadow: a Large-Scale Experimental Study. *Coast. Eng.* 73, 71–83. doi:10.1016/j.coastaleng.2012.10.007
- Lara, J. L., Maza, M., Ondiviela, B., Trinogga, J., Losada, I. J., Bouma, T. J., et al. (2016). Large-scale 3-D Experiments of Wave and Current Interaction with Real Vegetation. Part 1: Guidelines for Physical Modeling. *Coast. Eng.* 107, 70–83. doi:10.1016/j.coastaleng.2015.09.012
- Lei, J., and Nepf, H. (2019). Wave Damping by Flexible Vegetation: Connecting Individual Blade Dynamics to the Meadow Scale. *Coast. Eng.* 147, 138–148. doi:10.1016/j.coastaleng.2019.01.008
- Lemmen, D. S., Warren, F. J., James, T. S., and Mercer Clarke, C. S. L. (2016). *Canada's Marine Coasts in a Changing Climate*. Ottawa: Government of Canada.
- Lieske, D. J., and Bornemann, J. (2012). *Coastal Dykelands in the Tanramar Area: Impacts of Climate Change on Dyke Erosion and Flood Risk*. Canada: Mount Allison University.
- Lightbody, A. F., and Nepf, H. M. (2006). Prediction of Velocity Profiles and Longitudinal Dispersion in Salt Marsh Vegetation. *Limnol. Oceanogr.* 51 (1), 218–228. doi:10.4319/lo.2006.51.1.0218
- Losada, I. J., Maza, M., and Lara, J. L. (2016). A New Formulation for Vegetation-Induced Damping under Combined Waves and Currents. *Coast. Eng.* 107, 1–13. doi:10.1016/j.coastaleng.2015.09.011
- Markov, A. (2021). *Nature-based Solutions for Coastal Erosion Protection Literature Review*. Ottawa, Canada: University of Ottawa.
- Maza, M., Lara, J. L., and Losada, I. J. (2019). Experimental Analysis of Wave Attenuation and Drag Forces in a Realistic Fringe Rhizophora Mangrove Forest. *J. Adv. Water. Resour.* 131, 103376. doi:10.1016/j.advwatres.2019.07.006
- Maza, M., Lara, J. L., Losada, I. J., Ondiviela, B., Trinogga, J., and Bouma, T. J. (2015). Large-scale 3-D Experiments of Wave and Current Interaction with Real Vegetation. Part 2: Experimental Analysis. *Coast. Eng.* 106, 73–86. doi:10.1016/j.coastaleng.2015.09.010
- Mendez, F. J., and Losada, I. J. (2004). An Empirical Model to Estimate the Propagation of Random Breaking and Nonbreaking Waves over Vegetation Fields. *Coast. Eng.* 51, 103–118. doi:10.1016/j.coastaleng.2003.11.003
- Morris, R. L., Konlechner, T. M., Ghisalberti, M., and Swearer, S. E. (2018). From Grey to Green: Efficacy of Eco-Engineering Solutions for Nature-Based Coastal Defence. *Glob. Change Biol.* 24 (5), 1827–1842. doi:10.1111/gcb.14063
- Moudrak, N., Feltmate, B., Venema, H., and Osman, H. (2018). “Combating Canada's Rising Flood Costs: Natural Infrastructure Is an Underutilized Option,” in *Intact Centre on Climate Adaptation* (Canada: University of Waterloo).
- Muis, S., Apechechea, M. I., Dullaart, J., de Lima Rego, J., Madsen, K. S., Su, J., et al. (2020). A High-Resolution Global Dataset of Extreme Sea Levels, Tides, and Storm Surges, Including Future Projections. *Front. Mar. Sci.* 7, 263. doi:10.3389/fmars.2020.00263
- Narayan, S., Beck, M. W., Wilson, P., Thomas, C. J., Guerrero, A., Shepard, C. C., et al. (2017). The Value of Coastal Wetlands for Flood Damage Reduction in the Northeastern USA. *Sci. Rep.* 7 (1), 9463. doi:10.1038/s41598-017-09269-z
- Nepf, H. M. (1999). Drag, Turbulence, and Diffusion in Flow through Emergent Vegetation. *Water Resour. Res.* 35 (2), 479–489. doi:10.1029/1998wr900069
- Ozeren, Y., Wren, D. G., and Wu, W. (2014). Experimental Investigation of Wave Attenuation through Model and Live Vegetation. *J. Waterw. Port. Coast. Ocean Eng.* 140 (5). doi:10.1061/(asce)ww.1943-5460.0000251
- Percy, J. A. (2000). *Salt Marsh Saga: Conserving Fundy's Marine Meadows*. Canada: Bay of Fundy Ecosystem Partnership.
- Piercy, C. D., Pontee, N., Narayan, S., Davis, J., and Meckley, T. (2021). “Chapter 10: Coastal Wetlands and Tidal Flats,” in *International Guidelines on Natural and Nature-Based Features for Flood Risk Management*. Editors T. S. Bridges, J. K. King, J. D. Simm, M. W. Beck, G. Collins, Q. Lodder, et al. (Vicksburg, Mississippi, United States: U.S. Army Engineer Research and Development Center). MS.
- Pinsky, M. L., Guannel, G., and Arkema, K. K. (2013). Quantifying Wave Attenuation to Inform Coastal Habitat Conservation. *Ecosphere* 4 (8), 95. doi:10.1890/es13-00080.1
- Pontee, N., Narayan, S., Beck, M. W., and Hosking, A. H. (2016). Nature-based Solutions: Lessons from Around the World. *Proc. Institution Civ. Eng. - Marit. Eng.* 169 (1), 29–36. doi:10.1680/jmaen.15.00027
- Shepard, C. C., Crain, C. M., and Beck, M. W. (2011). The Protective Role of Coastal Marshes: A Systematic Review and Meta-Analysis. *PLoS One* 6 (11), e27374. doi:10.1371/journal.pone.0027374
- Sherren, K., Bowron, T., Graham, J. M., Rahman, H. M. T., and van Proosdij, D. (2019). “Coastal Infrastructure Realignment and Salt Marsh Restoration in Nova Scotia, Canada,” in *Responding to Rising Seas: Comparing OECD Countries' Approach to Coastal Adaptation* (Paris, France: Organization for Economic Collaboration and Development), 75–108.
- Sonnenwald, F., Stovin, V., and Guymer, I. (2019). Estimating Drag Coefficient for Arrays of Rigid Cylinders Representing Emergent Vegetation. *J. Hydraulic Res.* 57 (4), 591–597. doi:10.1080/00221686.2018.1494050
- Spalding, M. D., McIvor, A. L., Beck, M. W., Koch, E. W., Möller, I., Reed, D. J., et al. (2014). Coastal Ecosystems: a Critical Element of Risk Reduction. *Conserv. Lett.* 7 (3), 293–301. doi:10.1111/conl.12074
- Sutton-Grier, A. E., Wovk, K., and Bamford, H. (2015). Future of Our Coasts: the Potential for Natural and Hybrid Infrastructure to Enhance the Resilience of Our Coastal Communities, Economies and Ecosystems. *Environ. Sci. Policy* 51, 137–148. doi:10.1016/j.envsci.2015.04.006
- Sutton-Grier, A., Gittman, R., Arkema, K., Bennett, R., Benoit, J., Blich, S., et al. (2018). Investing in Natural and Nature-Based Infrastructure: Building Better along Our Coasts. *Sustainability* 10 (2), 523. doi:10.3390/su10020523

- Tinoco, R. O., San Juan, J. E., and Mullarney, J. C. (2019). Simplification Bias: Lessons from Laboratory and Field Experiments on Flow through Aquatic Vegetation. *J. Earth Surf. Process. Landforms* 45, 121–143. doi:10.1002/esp.4743
- Van der Meer, J. W., Allsop, N. W. H., Bruce, T., De Rouck, J., Kortenhaus, A., Pullen, T., et al. (2018). *EurOtop Manual on Wave Overtopping of Sea Defences and Related Structures. An Overtopping Manual Largely Based on European Research, but for Worldwide Application*. EurOtop. www.overtopping-manual.com.
- van Proosdij, D., Perrott, B., and Carrol, K. (2013). Development and Application of a Geo-Temporal Atlas for Climate Change Adaptation in Bay of Fundy Dykelands. *J. Coast. Res.* 65, 1069–1074. doi:10.2112/si65-181.1
- van Veelen, T. J., Fairchild, T. P., Reeve, D. E., and Karunarathna, H. (2020). Experimental Study on Vegetation Flexibility as Control Parameter for Wave Damping and Velocity Structure. *J. Coast. Eng.* 157, 103648. doi:10.1016/j.coastaleng.2020.103648
- Virgin, S. D., Beck, A. D., Boone, L. K., Dykstra, A. K., Ollerhead, J., Barbeau, M. A., et al. (2020). A Managed Realignment in the Upper Bay of Fundy: Community Dynamics during Salt Marsh Restoration over 8 Years in a Megatidal, Ice-Influenced Environment. *J. Ecol. Eng.* 149, 105713. doi:10.1016/j.ecoleng.2020.105713
- Vuik, V., Jonkman, S. N., Borsje, B. W., and Suzuki, T. (2016). Nature-based Flood Protection: the Efficiency of Vegetated Foreshores for Reducing Wave Loads on Coastal Dikes. *Coast. Eng.* 116, 42–56. doi:10.1016/j.coastaleng.2016.06.001
- Vuik, V., Van Vuren, S., Borsje, B. W., van Wesenbeeck, B. K., and Jonkman, S. N. (2018). Assessing Safety of Nature-Based Flood Defenses: Dealing with Extremes and Uncertainties. *Coast. Eng.* 139, 47–64. doi:10.1016/j.coastaleng.2018.05.002
- Webb, B., Douglass, S., Dix, B., and Asam, S. (2018). *Nature-based Solutions for Coastal Highway Resilience*. Report FHWA-HEP-18-037. Washington, DC: U.S. Federal Highway Administration (Accessed February 13, 2018).
- Wu, W.-C., and Cox, D. T. (2015). Effects of Vertical Variation in Vegetation Density on Wave Attenuation. *J. Waterw. Port. Coast. Ocean. Eng.* 142 (2). doi:10.1061/(ASCE)WW.1943-5460.0000326
- Wu, W.-C., and Cox, D. T. (2015). Effects of Wave Steepness and Relative Water Depth on Wave Attenuation by Emergent Vegetation. *Estuar. Coast. Shelf Sci.* 164, 443–450. doi:10.1016/j.ecss.2015.08.009
- Wu, W.-C., Ozeren, Y., Wren, D., Chen, Q., Zhang, G., Holland, M., et al. (2011). Phase I Report for SERRI Project No. 80037: Investigation of Surge and Wave Reduction by Vegetation, SERRI Report 80037-01, (Accessed January 16, 2011)
- Conflict of Interest:** The authors declare that the research was conducted in the absence of any commercial or financial relationships that could be construed as a potential conflict of interest.
- Publisher's Note:** All claims expressed in this article are solely those of the authors and do not necessarily represent those of their affiliated organizations, or those of the publisher, the editors and the reviewers. Any product that may be evaluated in this article, or claim that may be made by its manufacturer, is not guaranteed or endorsed by the publisher.

Copyright © 2022 Baker, Murphy, Cornett and Knox. This is an open-access article distributed under the terms of the Creative Commons Attribution License (CC BY). The use, distribution or reproduction in other forums is permitted, provided the original author(s) and the copyright owner(s) are credited and that the original publication in this journal is cited, in accordance with accepted academic practice. No use, distribution or reproduction is permitted which does not comply with these terms.